Model-Based Defect Recognition by 3-Dimensional Sparse Ultrasonic Arrays

Bernhard Menz

University of Karlsruhe, Institut für Meß- und Regelungstechnik, P.O.Box 6980,
76128 Karlsruhe, Germany, Email: menz@mrt.mach.uni-karlsruhe.de

Abstract - In this paper, a new technique for defect imaging is presented being able to distinguish between several defect shapes and producing an accurate image with small expense of hardware and time. High efficiency of the procedure is achieved by utilizing a priori information about the reflector models in the reconstruction algorithm. The main requirement for applying this technique is a limited number of possible defect shapes, each of which can be described by a sufficiently simple geometric model. By applying 1-, 2- or 3-dimensional arrays with few transmitters and receivers it is possible to obtain the required information by few measurements. A model-based reconstruction algorithm adapted to the specific measurement problem enables the classification of the defects and the estimation of the corresponding model parameters.

I INTRODUCTION

High-resolution techniques for ultrasonic inspection of material (e.g. tomography, holography, ALOK) generally require a great expense of sensorics and measurement time [1-3]. On the other hand, simple methods (e.g. A-, B-Scan without further reconstruction) usually provide only limited information about the defects, e.g. position and approximate size, or their application is restricted to examination of defects with one particular shape [4-6]. Given an expected image quality, for many applications the expense of the measuring system can be reduced by modeling the possible defects and by utilizing this a priori information in the reconstruction algorithm. A geometrical modeling essentially based on the shape of the defects proved to be suitable due to its simplicity and flexibility. Such a model in a simple form has already been successfully applied in robotics applications of ultrasound [7,8]. Within this article it is extended and adapted to applications of nondestructive testing. In contrast to conditions so far, no general restrictions exist on the parameter range of the defects as well as on the maximum number of transducers and their arrangement in the array, enabling a wider field of applications.

II 3-DIMENSIONAL SPARSE ARRAYS

In order to receive the required information from the specimen, a sparse array operating in impulse echo mode is located on its surface. The array may be implemented with synthetic array techniques or, as only few transducers are needed, by means of a real array of fixed transmitters and receivers. Due to the generally applicable principle of the reconstruction algorithm described below, the arrangement of the transmitters and receivers can be easily adapted to the shape of the specimen to be examined and to the types of expected defects which leads to great

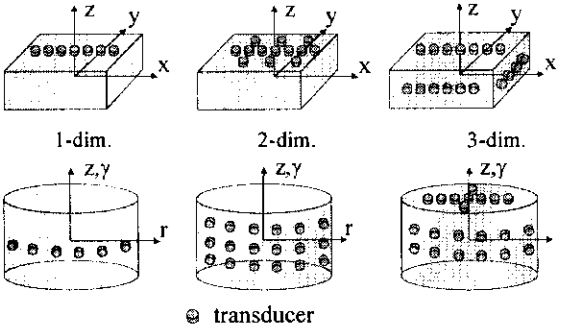

Fig. 1: Adapted sparse arrays.

flexibility of the measurement system. Examples of the adaptability of 1-, 2- and 3-dimensional arrays are shown in Fig. 1 for rectangular and cylindrical

0-7803-3615-1/96/$5.00

specimens. More complicated parts can be inspected without additional expense.

III DEFECT MODELS

In many practical applications the number of possible defect types is strongly limited. Provided that the defects may be approximated by simple geometrical classes, they can be described by a model of virtual transmitters. The virtual transmitter $T_{V_{ij}}{}^{k}$ describes the effect of the ultrasonic field originating from the i-th real transmitter T and influenced by the k-th defect D upon the j-th receiver. Thus the specimen can be alternatively described by the real defects or approximately by the set of all virtual transmitters. Fig. 2 demonstrates models of simple point (a), line (b), plane (c) and ellipsoid (d) defects. Extensions of

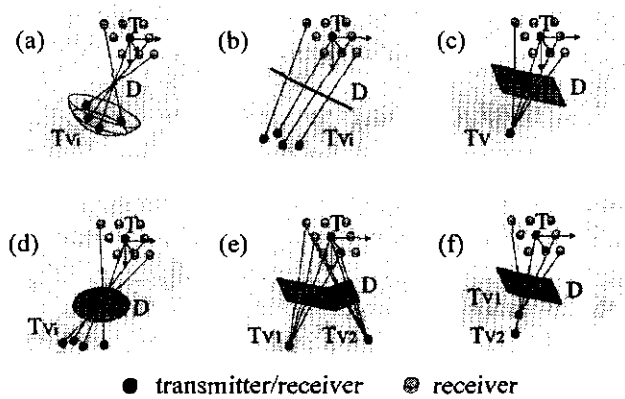

Fig. 2: Modeling defects by virtual transmitters T_V.

these models enable the description of geometrically more complicated defects (e) and the consideration of other defect parameters like the defect roughness (f) or the detection of interfaces with a negative gradient of the acoustic impedance [9]. Each defect model ω is defined by a system of generally non-linear equations

$$\mathbf{g}_{\omega}(\mathbf{M}_m, \mathbf{R}_m) = \mathbf{0}, \qquad (1)$$

where the vector $\mathbf{M}_m$ includes the parameters of the model and $\mathbf{R}_m$ includes the theoretical (relevant) parameters of the received impulses which correspond to the defect. With simple geometrical models, Eq. (1) is derived from the relation between defect parameters, location of the virtual transmitters and the arrangement of the receivers [10]. For simplicity, total reflection is assumed and diffraction effects due to the boundaries and local curvatures of the defects are neglected. Thus, the relative positions of the virtual transmitters contain the information on the defect type; the absolute location and the parameters of the virtual transmitters describe parameters (location, orientation, characteristics) of the defects.

IV MEASURING SYSTEM AND RECONSTRUCTION ALGORITHM

Due to the models introduced, the measuring process can be reduced to the determination of type and location of virtual transmitters, which, by the reconstruction algorithm, are assigned to the individual defects. Fig. 3 schematically shows the principle of the measuring system. From the received signals $r_i(t)$ which are components of the vector

$$\boldsymbol{r}(t) = \left(r_1(t), r_2(t), \ldots, r_{n_R}(t)\right)^T \qquad (2)$$

the relevant parameters $\boldsymbol{R}$ are extracted.
Assuming that the relevant information of each received signal is included in few parameters, the dataset and therefore the expense of the following reconstruction algorithm can be reduced strongly without reducing necessarily the quality of the reconstruction result. In the following we use the

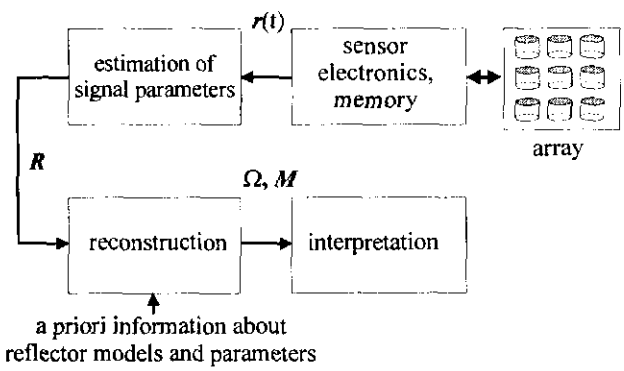

Fig. 3: Measuring system.

times of flight τ_{ij} and the amplitudes a_{ij} of the received impulses as components of the matrices

$$\boldsymbol{R}_{\tau} = (\tau_{ij}),\ \boldsymbol{R}_{a} = (a_{ij}), \qquad (3)$$

where index i relates to the i-th receiver and index j to the j-th echo. The signals received from a speci-

men with 3 simple defects (1 transmitter, 3 receivers) and the corresponding extracted parameters are shown in Fig. 4. The reconstruction process consists of 3 tasks:

I. Assignment of the impulses to the n_D individual defects,

II. Determination of the defect models
$\Omega = (\omega_1, \omega_2, ..., \omega_{n_D})$ (e.g. point, plane),

III. Estimation of the model parameters
$\boldsymbol{M} = (\boldsymbol{m}_1, \boldsymbol{m}_2, ..., \boldsymbol{m}_{n_D})$ (e.g. location, orientation).

Provided that the steps I-III can be solved separately, the problem can be significantly simplified. For example the problem of correspondence (I) can be solved separately, if the individual defects are located sufficiently apart. In this case, the pulses can be easily assigned to their corresponding defects by

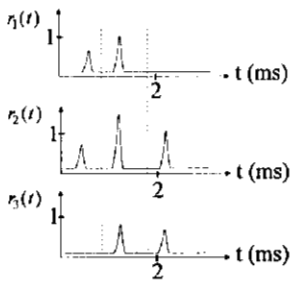

$$\boldsymbol{R}_\tau = \begin{vmatrix} 0.538 & 1.244 & - \\ 0.529 & 1.200 & 2.102 \\ 1.333 & 2.036 & - \end{vmatrix} \; [ms]$$

$$\boldsymbol{R}_a = \begin{vmatrix} 0.590 & 1.010 & - \\ 0.613 & 1.792 & 1.050 \\ 0.812 & 0.742 & - \end{vmatrix} \; [-]$$

Fig. 4: Received signals and extracted parameters.

their times of flight as shown in Fig. 4. This assignment, as well as all other methods which separate the computation of tasks I-III, requires severe restrictions on the measuring system and so they are useless for a universally applicable solution.

Generally the tasks I-III are coupled and therefore they have to be computed jointly. Due to the incorrect estimation of $\boldsymbol{R}$ and deviations from the ideal defect models, a stochastical approach has to be applied to solve the problem successfully. The maximum of the a posteriori probability $p(\Omega, \boldsymbol{M}|\boldsymbol{R})$ of the assumed defect models Ω and the model parameters $\boldsymbol{M}$, given the signal parameters $\boldsymbol{R}$, yields the defects [11]:

$$p_{I,0} = \max\{p(\Omega, \boldsymbol{M}|\boldsymbol{R})\} \Rightarrow \overline{\Omega}, \overline{\boldsymbol{M}} \qquad (4)$$

With a high number n_I of received impulses, the solution of the inverse problem, which corresponds with the multidimensional optimization of Eq. (4) is numerically exhaustive. In particular the solution is complicated because the number of defects, i.e. the dimensions of Ω and $\boldsymbol{M}$, are a priori unknown. Therefore the maximum a posteriori estimation (MAP) is reduced to combinations C_i of $n_{J,0}$ impulses,

$$n_{\min} \le n_{J,0} \le n_I \;, \qquad (5)$$

with the corresponding parameters $\boldsymbol{r}_0$ and the consideration of one defect of unknown type ω with the corresponding model parameters $\boldsymbol{m}$:

$$p_{J,0} = \max\{p(\omega, \boldsymbol{m}|\boldsymbol{r}_0)\} \qquad (6)$$

$$\text{with} \quad p(\omega, \boldsymbol{m}|\boldsymbol{r}_0) = \frac{p(\boldsymbol{r}_0|\omega, \boldsymbol{m}) \cdot p(\omega, \boldsymbol{m})}{p(\boldsymbol{r}_0)} \;. \qquad (7)$$

$p(\boldsymbol{r}_0|\omega, \boldsymbol{m})$ describes the error probability of the signal parameter estimation and of the modeling of the defects. The a priori information $p(\omega, \boldsymbol{m})$ consists of the a priori probability of the models and their parameters $p_{ap}(\omega, \boldsymbol{m})$ and of the detectability of the defect $d_{ap}(\omega, \boldsymbol{m})$,

$$p(\omega, \boldsymbol{m}) \sim p_{ap}(\omega, \boldsymbol{m}) \cdot d_{ap}(\omega, \boldsymbol{m}) \;. \qquad (8)$$

A binary definition of $d_{ap}(\omega, \boldsymbol{m})$, which depends on the specific array configuration and on the transducer characteristics,

$$d_{ap}(\omega, \boldsymbol{m}) = \begin{cases} 1, \text{ if detectable by all } n_{J,0} \text{ imp.} \\ 0, \text{ otherwise} \end{cases}, \qquad (9)$$

simplifies the reconstruction by reducing the number of meaningful combinations C_i. The minimum number of impulses $n_{\min}$ depends on the defect models and prevents trivial ambiguities ($p_{J,0} = 1$ for more than one defect class) within the solution of Eq. (6) by ensuring overdetermination of Eq. (1). If $p_{J,0}$ is smaller than the given threshold $p_{MIN,0}$, the combination of the $n_{J,0}$ impulses is rejected. If $p_{J,0}$ equals or exceeds $p_{MIN,0}$ a defect is assumed and the class $\omega_{\max}$ that maximizes $p_{J,0}$ is selected:

$$\begin{aligned} &p_{J,0} < p_{MIN,0}\text{: } CO_i \text{ rejected} \\ &p_{J,0} \ge p_{MIN,0}\text{: } CO_i \text{ accepted, } \omega = \omega_{\max} \end{aligned} \qquad (10)$$

Subsequently the assignment of impulses to the in-

dividual defects is expanded by increasing the number of combined impulses for the accepted defects and by using the corresponding signal parameters $\boldsymbol{r}_n$ to estimate the defect parameters until

$$p_{J,n} = \max\{p(\omega, \boldsymbol{m}|\boldsymbol{r}_n)\} < p_{MIN,n} \ . \qquad (11)$$

The estimation and the detection of Eq. (6) and Eq. (10) are applied to all combinations C_i (excluding the impulses which are already used in the determination of accepted defects). The combination of all accepted defects is finally filtered by joining defects with identical class and approximately the same parameters and by eliminating geometrical contradictions (e.g. a point which was detected behind a plane). By strongly limiting or skipping the increase of n_J by Eq. (11) the expense of the reconstruction algorithm can be reduced (which generally leads to decreased accuracy within the estimation of the defect parameters).

Within the reconstructions of Sec. V, $p(\boldsymbol{r}_\theta|\omega, \boldsymbol{m})$ is reduced to the probability of the deviation between the estimated TOF $\boldsymbol{r}_\tau$ and the theoretical values $\boldsymbol{r}_{\tau,m}$ which are determined by Eq. (1). These errors are assumed to be uncorrelated zero mean gaussian with variance $\sigma_\tau{}^2 = E\{(\boldsymbol{r}_{\tau,m} - \boldsymbol{r}_\tau)^t(\boldsymbol{r}_{\tau,m} - \boldsymbol{r}_\tau)\}$:

$$p(\boldsymbol{r}_\tau|\boldsymbol{m},\omega) = (2\pi\sigma_\tau{}^2)^{-\frac{n_J}{2}} \exp\Big(-\frac{1}{2\sigma_\tau{}^2}(\boldsymbol{r}_{\tau,m} - \boldsymbol{r}_\tau)^t(\boldsymbol{r}_{\tau,m} - \boldsymbol{r}_\tau)\Big) \ . \qquad (12)$$

The applied a priori information on the models exists of a limited set Ω_{ap} of possible defect models and a limited range $M_{ap}(\omega)$ of possible, uniformly distributed model parameters :

$$p_{ap}(\omega, \boldsymbol{m}) = p(\boldsymbol{m}|\omega) \cdot p(\omega) \ , \qquad (13)$$

$$\text{with} \quad p(\boldsymbol{m}|\omega) \sim \begin{cases} 1, \boldsymbol{m} \in M_{ap}(\omega) \\ 0, otherwise \end{cases} \ , \qquad (14)$$

$$p(\omega) \sim \begin{cases} 1, \omega \in \Omega_{ap} \\ 0, otherwise \end{cases} \ . \qquad (15)$$

$p(\boldsymbol{r}_0)$ is considered to be constant, which generally is a good approximation if the standard deviation σ_τ of the measurement errors is small compared to the possible parameter range of $\boldsymbol{r}_{\tau,m}$. Further details of the reconstruction algorithm and the specification of $p_{MIN,n}$ can be found in [12].

V MEASUREMENTS

The performance of the method is demonstrated by measurements with cubes of polymeric methylmetacrylate (Perspex) and steel. The cubes contain artificial defects: cylindrical holes of different diameter (steel, d = 2, 20 mm; Fig. 5 S.I), respectively point and plane shaped aluminium defects (Perspex, point: small circular discs, d=5mm, planes: a=20mm, b=30mm; Fig. 5 S.II). Sparse arrays of few transmitters and receivers with wide angle radiation patterns ($f_0 = 2\text{MHz}$, $\varphi_0 = \pm 30°$) where

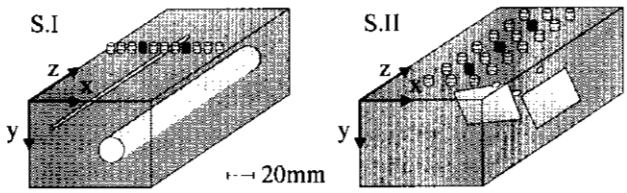

Fig. 5: Specimens.

contacted with the specimen. The different 1- or 2-dimensional array realizations in Fig. 5 follow from the extent of the defect classes under examination and demonstrate the flexibility of the method.

The applied a priori information on the defect models within specimen S.I is the cylindrical defect shape and the uniform orientation of the cylinders parallel to the z-axis. With $n_{J,0} = n_{\min} = 4$ and a 1-dimensional array, both cylinders are detected but the location as well as the diameter of the large cylinder are reconstructed with a great error (Fig. 6-I). This error results from the 1-dimensional array con-

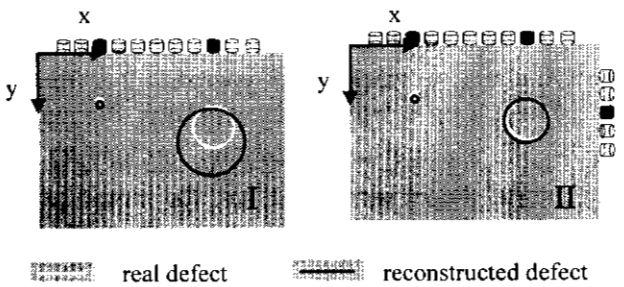

Fig. 6: Results of reconstruction.

figuration and can be reduced by extending the array to the second dimension, which increases the accu-

racy to $\pm 2mm$ (Fig. 6-II).

Within specimen S.II points and planes with arbitrary orientation and maximum dimensions of $a,b \leq 30\text{mm}$ are assumed. With the minimum number of impulses $n_{J,0} = n_{\min} = 4$ all defects are recognized, but one point is classified as a plane and one artifact plane is detected (Fig. 7). The false classification and the artifact are eliminated by combinations of $n_{J,0} = 5$ impulses. The defect parameters are determined within an accuracy of 2mm (location) and 5° (orientation). Using 6 impulses, two existing point defects are not detected, which

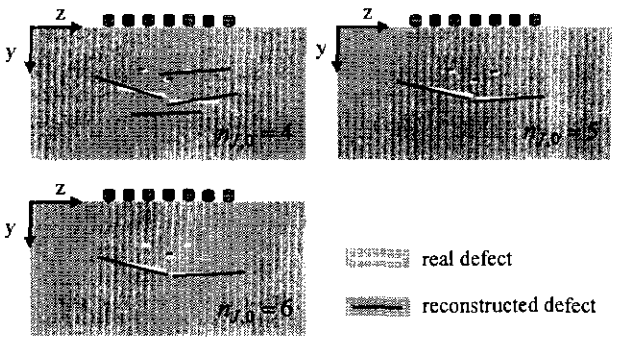

Fig. 7: Results of reconstruction.

results from the fact that only 5 impulses originating from each of the two missed point defects were received. This example demonstrates the importance of the n_J to the quality of the measurement (in particular to the probability of detection and the suppression of artifacts). The problem generally can be solved by applying a sufficient number of transducers and by starting with a small set of impulses (e.g. $n=n_{min}+1$) [12].

The standard deviation of the TOF estimation $\sigma_\tau \approx 1{,}2\,\text{mm}$ is much higher than the standard deviation of the TOF estimation with known reflector ($\sigma_{TOF} \approx 0.2\,\text{mm}$). Thus it is mainly determined by the approximations within the modeling which neglects the diffraction due to the boundary and the local curvature of the defects. If in addition to these approximations, deviations from the assumed models appear (e.g. slightly uneven "planes"), σ_τ increases further. So it may be advantageous to apply an extended model which includes or at least approximates the deviations.

These errors of the modeling, together with the increasing expense of reconstruction with growing number of reflectors, seems to be the main limits of the method. But if the accuracy of the modeling is sufficient exact and the number of reflectors is small, the measuring system enables an effective reduction of expense of measuring time and hardware. Due to the advantages and restrictions, the technique seems to be particularly suitable for time critical applications like real-time 100% product testing or examinations of very large objects.

REFERENCES

[1] Berkhout, A.J.: *Resolution Limits of Acoustical Echo Systems.* Acoustical Imaging Vol. 14, Plenum Press; New York 1986, pp. 19-31.

[2] Langenberg, K.J.; Brück, D.; Fischer, M.: *Invers Scattering Algorithms.* New Procedures in Nondestructive Testing, Springer Verlag 1983, pp. 381-391.

[3] Capineri, L.: *Time-of-flight Diffraction Tomography for NDT Applications.* Ultrasonics Vol. 30 No. 5 1992, pp. 275-288.

[4] Gericke, O.R.: *Determination of the Geometry of Hidden Defects by Ultrasonic Pulse Analysis Testing.* The J. of the Acoust. Soc. of America 35 3/1963, pp. 364-368.

[5] Sasaki, K.; Takano, M.: *Classification of Objects' Surface by Acoustic Transfer Function.* Proceedings of the 1995 IEEE/RSJ Intern. Conf. on Intelligent Robots ans Systems, Vol. 1, pp. 821-828.

[6] Yamani, A.; Al Akhdhar, S.Z.: *A Novel Technique for Defects Classification from their Ultrasonic Pulse Echoes.* Advances in Signal Processing for Nondestructive Evaluation of Materials, Kluwer Acad. Pub. (1994), pp. 371-384.

[7] Kleeman, L.; Kuc, R.: *Mobile Robot Sensor for Target Localization and Classification.* The Intern. Journal of Robotics Research, Vol. 14 No. 4 (1995), pp. 295-318.

[8] Peremans, H.; Audenaert, K.; Van Campenhout, J.M.: *A High-Resolution Sensor Based on Tri-aural Perception.* IEEE Trans. on Robotics and Automation, Vol. 9 No. 1 (1993), pp. 36-48.

[9] Ogilvy, J.A.: *Model for the Ultrasonic Inspection of Rough Defects.* Ultrasonics, Vol. 27 (1989), pp. 69-79.

[10] Menz, B.: *Ultraschallarrays zur modellbasierten Objekterkennung.* Sensoren und Meßsysteme, VDI-Berichte 1255 (1996), pp. 357-362.

[11] Van Trees, H.L.: *Detection, Estimation, and Modulation Theory, Part I,* JohnWiley & Sons Inc. New York (1968)

[12] Menz, B.: *Model-Based Object Recognition by 3-Dimensional Sparse Arrays.* To be published: Acoustical Imaging, Vol. 23, Plenum Press, New York (1997)